SAFETY MARGINS AFTER FAILURE OF FUEL CLADDING DURING PROTECTED LOSS-OF-HEAT-SINK ACCIDENTS IN A SODIUM-COOLED FAST REACTOR

Yoshitaka FUKANO, Masahiro NISHIMURA and Fumiaki YAMADA
Plant Safety Evaluation Department,
Sector of Fast Reactor Research and Development,
Japan Atomic Energy Agency
1 Shiraki, Tsuruga-shi, Fukui 919-1279, Japan
fukano.yoshitaka@jaea.go.jp

ABSTRACT

Protected loss-of-heat-sink (PLOHS) events are identified as one of the most dominant sequences in a sodium-cooled fast reactor. Safety margins for significant core damage in PLOHS events were therefore studied in this paper assuming fuel cladding failure.

The following three possible mechanisms leading to degradation of the core were then identified to be scrutinized by a thorough and state-of-the-art review of open papers on the phenomena anticipated to occur under cladding failure conditions:

(1) Fuel melting due to fuel-sodium reaction product (FSRP) formation,
(2) Thermal transient due to FP gas impingement from adjacent failed fuel pins, and
(3) Mechanical load due to the same FP gas impingement.

Following results were thus obtained through simulation analyses on each phenomenon mentioned above using the FUCALF code:

(1) No fuel melting occurs due to FSRP formation,
(2) No fuel melting occurs due to FP gas impingement from adjacent failed fuel pins, and
(3) No mechanical pin failure occurs due to the same FP gas impingement.

Moreover, these are valid at the coolant temperatures of up to 950 degree C. It was therefore concluded that large safety margins are provided during PLOHS events even in failure of fuel cladding. These results will be effectively used in formulating the safety criteria for SAs or BDBAs as one of the supporting evidences to be seriously considered.

KEYWORDS
Sodium-cooled fast reactor (SFR),
Protected loss of heat sink (PLOHS),
Severe accident (SA),
Beyond design-basis accident (BDBA)

1. INTRODUCTION

The following safety criteria for anticipated operational occurrences are commonly and uniformly employed for all the DBAs in the Japanese prototype sodium-cooled fast reactor (Monju) to prevent fuel melting and cladding failure [1], although specific safety criteria are defined for each design basis accident (DBA) to prevent significant core damage:

(a) Maximum fuel temperature shall be below the melting point,

(b) Maximum cladding temperature shall be below 830 degree C in order to prevent cladding failure, and

(c) Maximum coolant temperature shall be below the boiling point.

Cladding failure is allowed, on the contrary to that, in beyond DBAs (BDBAs) or severe accidents (SAs), whereas the core cooling capability is also needed to be secured as in DBAs. No fuel melting enables this by keeping the core in a coolable geometry, and is thus conservatively required even under such a condition.

A past study has already clarified the accident sequences beyond design basis to be assessed when confirming the effectiveness of countermeasures against SAs for the reactor in question [2]. Figure 1 shows evaluated core damage frequency assuming only the measures against DBAs and that assuming the measures against both DBAs and SAs. Protected loss-of-heat-sink (PLOHS) events are then identified as one of the most dominant sequences in both cases. Safety margins for significant core damage in PLOHS events were therefore studied in this paper assuming fuel cladding failure.

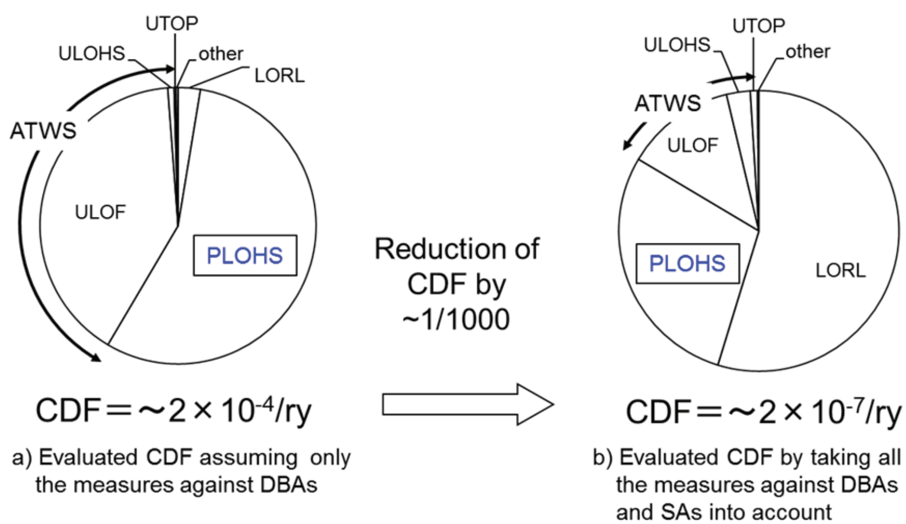

Figure 1. Accident sequence groups identified based on the internal event PRA

The following three possible mechanisms leading to degradation of the core were then identified in this study to be scrutinized by a thorough and state-of-the-art review of open papers on the phenomena anticipated to occur under cladding failure conditions:

(1) Fuel melting due to fuel-sodium reaction product (FSRP) formation,

(2) Thermal transient due to FP gas impingement from adjacent failed fuel pins, and

(3) Mechanical load due to the same FP gas impingement.

All the evaluation models mentioned above have been incorporated into the FUCALF code (FUel pin Condition Analysis code at Local Fault) by developing needed but missing some methods in this study.

Safety margins are studied during PLOHS events even in failure of fuel cladding through analyses on each phenomenon mentioned above using the FUCALF code.

2. SAFETY EVALUATION METHODOLOGY ON CONSEQUENCES AFTER CLADDING FAILURES

Following three possible mechanisms of significant core damage due to cladding failure were identified from a thorough and state-of-the-art review of open papers in this study:

(1) Fuel melting due to FSRP formation,

(2) Thermal transient due to FP gas impingement from adjacent failed fuel pins, and

(3) Mechanical load due to the same FP gas impingement.

Although (2) thermal transient due to FP gas impingement can be analyzed by the FALL code [3-5] which was used in the safety assessment of the licensing of Monju, evaluation model for determining the duration of FP gas release was not included which is important for cladding creep failure. Furthermore evaluation models for (1) fuel melting due to FSRP formation, and (3) mechanical load due to FP gas impingement are also not incorporated to the FALL code. Therefore the FUCALF code which includes all the mathematical models to be described in the following sections was newly developed for the integrated analysis of consequences of cladding failures as an evolved version of the FALL code.

Table 1. Fuel pellet swelling rates due to FSRP measured in reference [7]

Sodium Temperature (degree C)	Heat transient time (h)	ΔD/D (%)
800	1	2.44
800	3	2.67
800	7	2.85
800	17	2.86
750	72	2.90
700	3	1.00
700	8	1.48
700	24	2.03
700	24	1.84
700	40	2.01
700	120	2.47
700	406	2.52
650	24	0.80
650	576	1.41
650	2565	1.71
600	24	0.45
600	72	0.48
600	675	0.56
600	3267	0.62
500	144	0.19
500	480	0.30
500	3500	0.30

2.1. Fuel Melting due to FSRP Formation and Subsequent Molten Fuel Ejection into the Coolant Channel

Low thermal conductivity of FSRP (Na_3MO_4) [6-11] may induce fuel melting of which the reactions are described by the following chemical equations.

$$MO_{2-x} + \frac{3(y-x)}{2+y} Na \Leftrightarrow \frac{y-x}{2+y} Na_3MO_4 + \frac{2+x}{2+y} MO_{2-y} \quad (1)$$

$$3Na + MO_{2-y} + \frac{1+y}{2} O_2 \Leftrightarrow Na_3MO_4 \quad (2)$$

Table 1 shows the fuel pellet swelling rates due to FSRP measured in the out-of-pile experiment [7]. The following swelling rate due to FSRP which gives a conservative value as shown in **Figs. 2 to 6** was introduced into the FUCALF code in this study based on the above-mentioned experiment.

$$\frac{\Delta D}{D} = \ln\left[(t_f + 0.5) \times (T_s - 195)\right] \times \frac{(T_s - 205)^3}{\alpha} \quad (3)$$

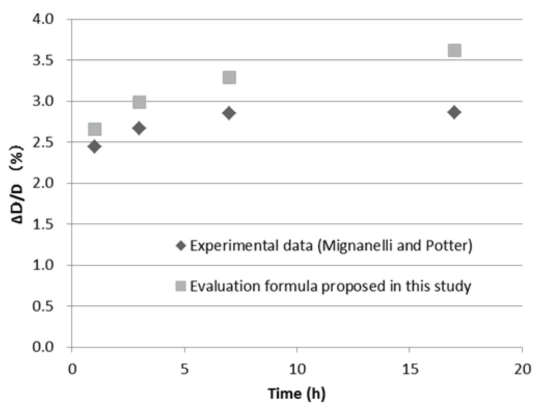

Figure 2. Fuel pellet diameter increase due to FSRP formation at 800 degree C

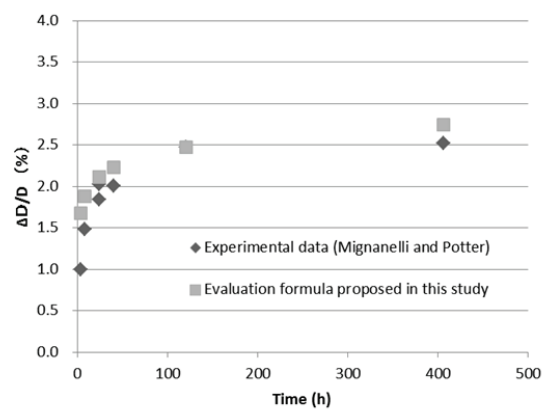

Figure 3. Fuel pellet diameter increase due to FSRP formation at 700 degree C

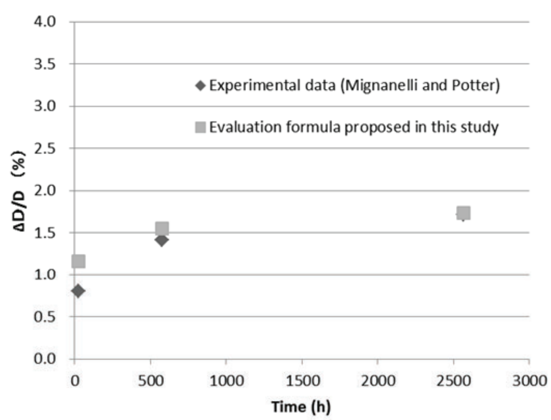

Figure 4. Fuel pellet diameter increase due to FSRP formation at 650 degree C

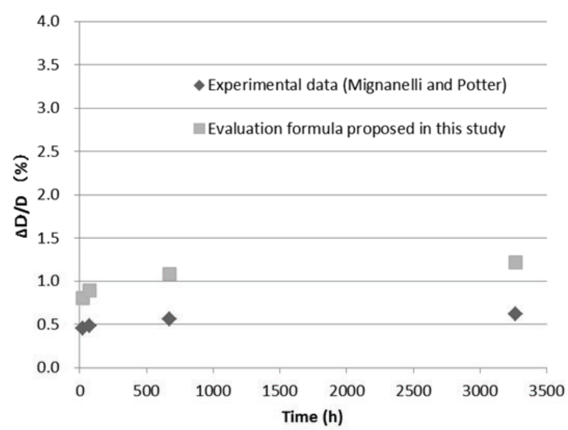

Figure 5. Fuel pellet diameter increase due to FSRP formation at 600 degree C

Temperature distribution within a fuel pin was calculated based on the following three-dimensional transient heat conduction equation [3,4] in the FALL code.

$$C_p \rho \frac{\partial T}{\partial t} = div(k \cdot gradT) + Q(z) \quad (4)$$

The heat conduction in the FSRP region was also incorporated into the FUCALF code in addition to those in the fuel, gap, cladding and coolant regions.

2.2. Thermal Transient due to FP Gas Impingement from Adjacent Failed Fuel Pin

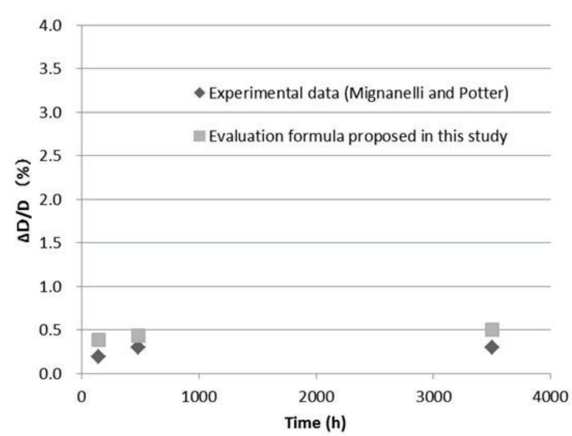

Figure 6. Fuel pellet diameter increase due to FSRP formation at 500 degree C

FP gas pressure in the fuel pins of SFRs can be larger than those of LWRs because fuel burnups in SFRs are generally higher than those in LWRs. Therefore thermal transients due to FP gas impingement from adjacent failed fuel pin have been historically studied [12-14].

Although the duration of FP gas release is also important in analyzing this kind of event, the evaluation model is not included in the FALL code as mentioned above. Cladding thermal creep depends not only on the cladding temperature but also on its duration. Therefore the following mathematical model [13] was implemented into the FUCALF code for calculating the duration of FP gas release (t_T).

$$t_T = t_S + t_E \tag{5}$$

where

$$t_S = \frac{1}{C_d \cdot C_\gamma \cdot \frac{A_0}{V} \cdot \sqrt{R' T_g}} \cdot \ln \frac{C_d \cdot P_g(0)}{P_S \cdot \left(\frac{\gamma+1}{2}\right)^{\frac{\gamma}{\gamma-1}}} \tag{6}$$

$$t_E = \frac{1}{C_d \cdot C_\gamma \cdot \frac{A_0}{V} \cdot \sqrt{R' T_g}} \cdot \ln \frac{P_{crit}}{P_S} \tag{7}$$

2.3. Mechanical Load due to FP Gas Impingement from Adjacent Failed Fuel Pin

Analysis of resonance oscillation of the fuel pin is necessary for that to be affected by a pressure pulse induced by the FP gas impingement from an adjacent failed fuel pin. The resonance oscillation will be evoked resulting in a possible fuel pin failure when the time period t_u during which the differential pressure across the fuel pin diameter is maintained is in the same order of the duration t_r which corresponds to the eigenfrequency of the fuel pin. Therefore the following mathematical model [13] was introduced into the FUCALF code for calculating the durations of t_u and t_r.

$$t_u = \frac{2D}{c} \tag{8}$$

$$t_r = \frac{2\pi l^2}{\beta_0^2} \sqrt{\frac{M_f}{EI}} \tag{9}$$

3. APPLICATION TO THE SAFETY EVALUATION OF MONJU

A safety evaluation after fuel cladding failure during PLOHS in Monju was performed using the above-mentioned methodology.

3.1. Fuel Melting due to FSRP Formation and Subsequent Molten Fuel Ejection into the Coolant Channel

The possible maximum duration of irradiation under the run-beyond-cladding-breach (RBCB) condition will be 740 days in Monju conservatively assuming that fuel pin failure occurs at the beginning of fuel life. The fuel pellet swelling ($\Delta D / D$) due to FSRP is estimated to be 9.4% at 883 degree C respectively after an irradiation of 17,760 hours (740 days) based on the equations described in Section 2.1. Therefore the fuel temperature was analyzed by the FUCALF code conservatively assuming that $\Delta D / D$ is 10%. The analytical conditions and results by the FUCALF code are presented in **Table 2** and **Figure 7**. The maximum fuel temperature was far below the fuel melting point despite a conservative $\Delta D / D$ was assumed.

Table 2. Main analytical conditions for fuel pin temperature with FSRP by FUCA code

Axial position of FSRP	Core mid-plane
Power density of fuel (W/cm^3)	120 (7% of nominal power)
Linear heat rating (W/cm)	27.6 (7% of nominal power)
Power density of FSRP (W/cm^3)	60.2 (7% of nominal power)
Thermal conductivity of FSRP	25% of fuel thermal conductivity
FSRP thickness	10% of fuel radius
Fuel-cladding gap conductance (W/cm^2/degree C)	0.405
Coolant temperature (degree C)	950
Number of axial cells	1
Number of radial cells	16
Fuel pellet	10
Fuel-Cladding gap	1
FSRP	1
Cladding	3
Coolant	1
Number of azimuthal cells	1

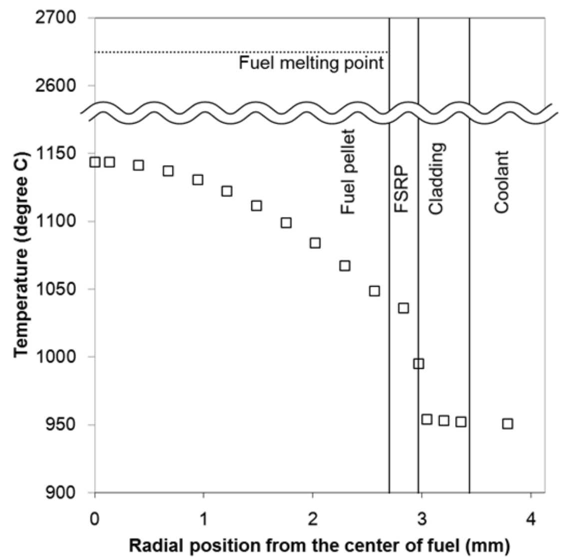

Figure 7. Temperature distribution from center of fuel pin with FSRP layer of which thickness is 10% of fuel radius

It should be noted that the fuel temperature in Figure 7 is moreover conservative because of the following reasons:

- Although the FSRP temperature in Figure 7 shows above the sodium saturation temperatures, FSRP will not form under such an above the saturation temperature condition [10];
- Although the fuel-cladding gap conductance used in the analysis is the value for under normal conditions as shown in **Figure 8** [5], it can be higher because of FSRP and sodium intrusion into the gap;

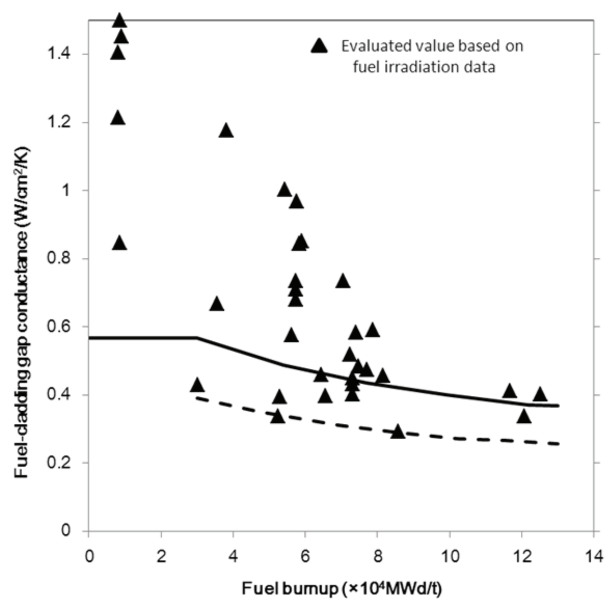

Figure 8. Fuel-cladding gap conductance cited from the Monju licensing

- Although the linear heat rating (LHR) in the analysis is assumed to be a constant value, the highest value at the beginning of irradiation including uncertainty, it will be decreased as fuel burnup increases in the actual reactor, Monju as shown in **Figure 9** [5].

Therefore fuel melting due to FSRP formation is highly unlikely in Monju.

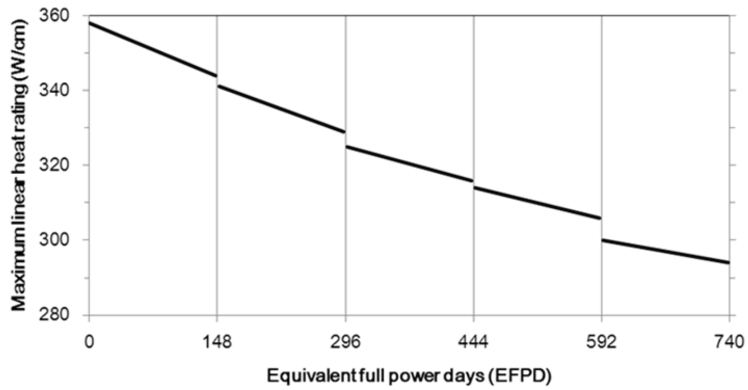

Figure 9. History of maximum linear heat rating

3.2. Thermal Transient due to FP Gas Impingement from Adjacent Failed Fuel Pin

Table 3 shows the main analytical conditions for the FUCALF code calculation. The effective heat transfer coefficient between released FP gas from the failed fuel pin and cladding of adjacent fuel pin were experimentally investigated [12-14] as shown in **Figure 10**. The minimum envelop value of 1.0 $W/cm^2/K$ was conservatively used in this study. A gas blanketing angle of 360 degrees was also considered conservatively in addition to 180 degree assuming multiple adjacent pin failures.

Table 3. Main analytical conditions for fuel pin temperature by FUCA code

Axial position of gas blanketing	Core mid-plane
Power density of fuel (W/cm^3)	120 (7% of nominal power)
Linear heat rating (W/cm)	27.6 (7% of nominal power)
Angles for gas blanketing (degree)	180, 360
Released gas temperature (degree C)	950
Fuel-cladding gap conductance (W/cm^2/degree C)	0.405
Coolant temperature (degree C)	950
Number of axial cells	1
Number of radial cells	15
Fuel pellet	10
Fuel-Cladding gap	1
FSRP	0
Cladding	3
Coolant	1
Number of azimuthal cells	
Sectors with gas blanketing	3 for 180degree 1 for 360degree
Sectors without gas blanketing	3 for 180degree 0 for 360degree

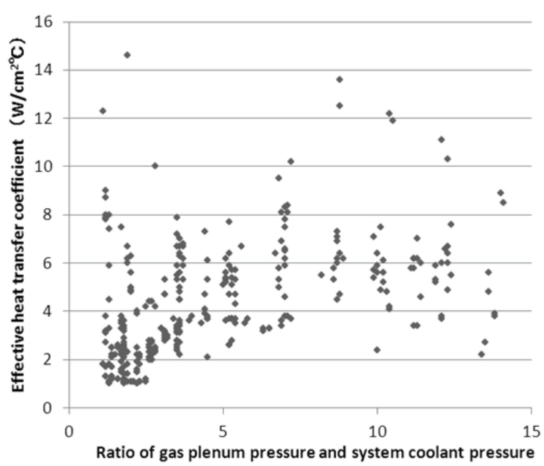

Figure 10. Effective heat transfer coefficient between released FP gas from the failed fuel pin and cladding of adjacent fuel pin

Figure 11 shows the temperature distribution from the center line of the fuel pin to the coolant or FP gas blanketing region analyzed by the FUCALF code. The maximum fuel temperature is below the melting point even at the peak power node (PPN).

Therefore fuel melting due to FP gas impingement from adjacent failed fuel pins is highly unlikely to occur in Monju.

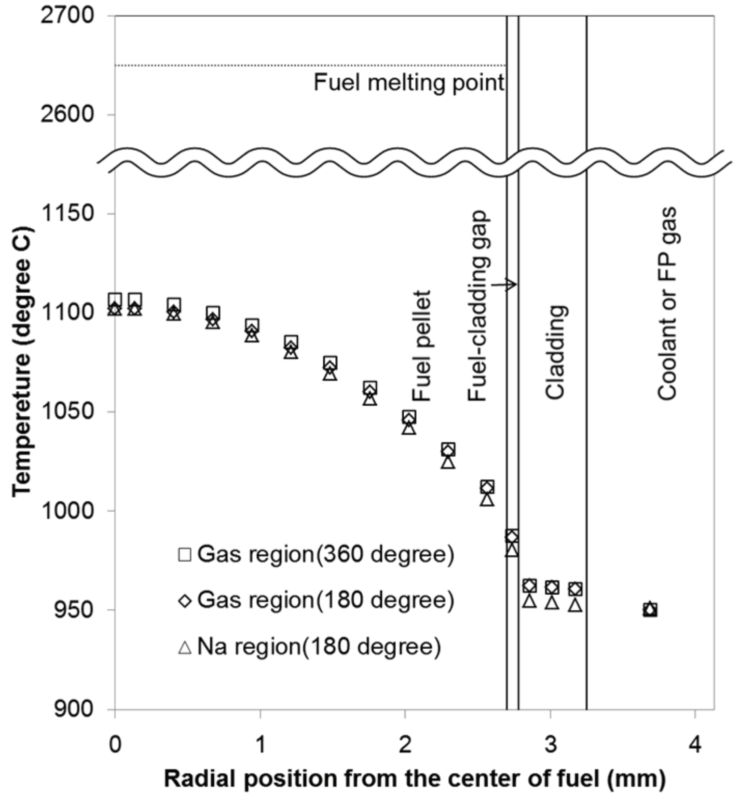

Figure 11. Temperature distribution from the center of fuel pin during FP gas release form adjacent fuel pins

3.3. Mechanical Load due to FP Gas Impingement from Adjacent Failed Fuel Pin

The main calculation conditions and results for the durations of t_u and t_r mentioned in Section 2.2 are shown in **Table 4**. Fuel pin failure due to resonance oscillation is highly unlikely in Monju because t_u is much smaller than t_r.

Table 4. Main analytical conditions and results for mechanical fuel pin failure by FUCA code

Analytical conditions	
Diameter of fuel pin (d) [m]	6.5×10^{-3}
Sonic velocity (c) [m/s]	2.3×10^{3}
Constant (β_0) [-] (simply-supported end conditions)	π
Length of fuel pins (unsupported) (l) [m]	3.0×10^{-1}
Mass of fuel pin per unit length (M) [kg/m]	7.1×10^{-2}
Elasticity modulus (E) [kg/m/s^2]	1.6×10^{11}
Moment of inertia (I) [m^4]	4.1×10^{-11}
Analytical results	
t_u [s]	5.7×10^{-6}
t_r [s]	6.0×10^{-3}

4. DISCUSSIONS

From all the results mentioned above in Chapter 3, fuel melting and mechanical fuel pin failure are highly unlikely. Furthermore no fuel melting occurs even assuming that FSRP formation and FP gas impingement from adjacent failed fuel pins are superposed. **Table 5** and **Figure 12** show main calculation conditions and results based on this assumption. The maximum fuel temperature is below the melting point.

Therefore the core cooling capability can be secured even after the fuel cladding failure during PLOHS event at least at the coolant temperatures of up to 950 degree C.

Table 5. Main analytical conditions for fuel pin temperature with FSRP during FP gas release form peripheral fuel pins by FUCA code

Axial position of gas blanketing	Core mid-plane
Power density of fuel (W/cm^3)	120(7% of nominal power)
Linear heat rating (W/cm)	27.6(7% of nominal power)
Power density of FSRP (W/cm^3)	60.2(50% of fuel power density)
Thermal conductivity of FSRP	25% of thermal conductivity of fuel
Angles for gas blanketing (degree)	180,360
Released gas temperature (degree C)	950
FSRP thickness (mm)	0.27(10% of fuel radius)
Fuel-cladding gap conductance (W/cm^2/degree C)	0.405
Coolant temperature (degree C)	950
Number of axial cells	1
Number of radial cells	16
Fuel pellet	10
Fuel-Cladding gap	1
FSRP	1
Cladding	3
Coolant	1
Number of azimuthal cells	
Sectors with gas blanketing	3 for 180degree 1 for 360degree
Sectors without gas blanketing	3 for 180degree 0 for 360degree

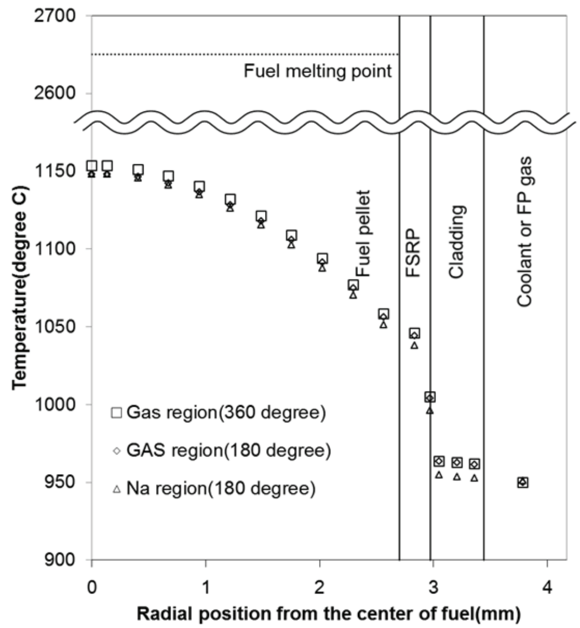

Figure 12. Temperature distribution from the center of fuel pin with FSRP layer of which thickness is 10% of fuel radius during FP gas release form adjacent fuel pins

5. CONCLUSIONS

The following three possible mechanisms leading to degradation of the core were identified to be scrutinized by a thorough and state-of-the-art review of open papers on the phenomena anticipated to occur under cladding failure conditions:

(1) Fuel melting due to fuel-sodium reaction product (FSRP) formation,
(2) Thermal transient due to FP gas impingement from adjacent failed fuel pins, and
(3) Mechanical load due to the same FP gas impingement.

All the evaluation models mentioned above have been incorporated into the FUCALF code by developing needed but missing some methods. Thus a safety assessment methodology after failure of fuel cladding failure which is applicable to arbitrary SFRs with different fuel and core designs has been provided in this study.

Furthermore following results were obtained through simulation analyses on each phenomenon mentioned above using the FUCALF code:

(1) No fuel melting occurs due to FSRP formation,
(2) No fuel melting occurs due to FP gas impingement from adjacent failed fuel pins, and
(3) No mechanical pin failure occurs due to the same FP gas impingement.

Moreover, these are valid at the coolant temperatures of up to 950 degree C. It was therefore concluded that large safety margins are provided during PLOHS events even in failure of fuel cladding in Monju.

These results will be effectively used in formulating the safety criteria for SAs or BDBAs as one of the supporting evidences to be seriously considered.

NOMENCLATURES

A_0 : Flow area of the cladding perforation (m^2)
c : Sonic velocity (m/s)
C_d : Equivalent discharge coefficient (-)
C_p : Specific heat at constant pressure (J/g/K)
C_v : Specific heat at constant volume (J/g/K)
C_γ : $= \sqrt{\gamma \cdot (\frac{2}{\gamma+1})^{\frac{\gamma+1}{\gamma-1}}}$ (-)
D : Fuel pellet diameter (m)
E : Elasticity modulus ($kg/m/s^2$)
H : Latent heat of vaporization (kJ/kg)
I : Moment of inertia (m^4)
k : Thermal conductivity (W/m/K)
l : Length of fuel pins (unsupported) (m)
M: = (U,Pu)
M_f : Mass of fuel pin per unit length (kg/m)
M_g : Molar mass of gas (kg/mol)
P_{crit} : $= \frac{P_S}{C_d} (\frac{\gamma+1}{2})^{\frac{\gamma}{\gamma-1}}$ (N/m^2)
$P_g(0)$: Gas plenum pressure before fuel pin failure (N/m^2)
P_S : System coolant pressure at the fission-gas release point (N/m^2)
Q : Power density (W/cm^3)
R : Ideal gas constant (J/kg/K)
R' : $= \frac{R}{M_g}$ (J/mol/K)
T : Temperature (K)
t : Time (s)
t_E : Duration of FP gas release under subsonic flow (s)
t_f : Time after fuel pin failure (h)
T_g : Gas plenum temperature (K)
t_r : duration which corresponds to the eigenfrequency of the fuel pin (s)
T_s : Sodium temperature at around the cladding defect (degree C)
t_S : Duration of FP gas release under supersonic flow (s)
t_T : Duration of FP gas release (s)
t_u : Time period during which the differential pressure across the fuel pin diameter is maintained (s)

V : Volume of gas plenum (m^3)
2-x: O/M ratio of fuel pellet at the beginning (-)
2-y: O/M ratio of fuel pellet at the chemical equilibrium (-)

Greek Letters

α : Constant ($=5.4\times10^8$ in case of T_s >675 and $=7.1\times10^8$ in case of $T_s \leq 675$) (-)

β_0 : Constant (= π for simply-supported end conditions or =4.73 for fixed-end conditions)

γ : Ratio of specific heat at constant pressure and constant volume $[=\dfrac{C_P}{C_V}]$ (-)

ρ : Density (g/m^3)

ACKNOWLEDGMENTS

The authors would like to express their gratitude to H. Akahori of NESI Inc. who assisted calculations using FUCALF code.

REFERENCES

1. Fukano Y, Development of safety assessment methodology on fuel element failure propagation in SFR and its application to Monju. J.Nucl.Sci.Technol., 2015; 52, 178-192.
2. Onoda Y, Kurisaka K, Sakai T, Identification of the Accident Sequences for the Evaluation of the Effectiveness of Severe Accident Measures on Prototype Sodium-Cooled Fast Reactor, Proc. Of NUTHOS-10; 2014 December 14-18; Okinawa(Japan).
3. Fukano Y, Comprehensive and consistent interpretation of local fault experiments and application to hypothetical local over-power accident in Monju. J.Nucl.Sci.Technol., 2013;50,950-965.
4. Nakai R, Itoh M, Terata K, Kani Y, Maeda K, Endo H, Kondo S, Aizawa K, Ohmori Y. Computer codes for safety analysis of LMFBR. Japan: Japan Atomic Energy Agency; PNC TN241 81-28; 1981 [in Japanese].
5. Japan Atomic Energy Agency. The licensing document for the construction permit of the prototype FBR Monju. Japan: Japan Atomic Energy Agency; 1980, revised 2006 [in Japanese].
6. Mignanelli MA, Potter PE, An investigation of the reaction between sodium and hyperstoichiometric urania. J.Nucl.Mat., 1983;114,168-180.
7. Mignanelli MA, Potter PE, The reactions between sodium and plutonia, urania-plutonia and urania-plutonia containing fission product simulant. J.Nucl.Mat., 1984;125,182-201.
8. Lorenzelli R, Athanassiadis T, Pascard R, Chemical reactions between sodium and $(U,Pu)O_2$ mixed oxides. J.Nucl.Mat., 1985;130,298-315.
9. Strain RV, Gross KC, Lambert JDB, Colburn RP, Odo T, Behavior of breached mixed-oxide fuel pins during off-normal high-temperature irradiation. Nucl. Technol., 1992; 97, 227-240.
10. Strain RV, Bottcher JH, Ukai S, Arii Y, Fuel-sodium reaction product and its influence on breached mixed-oxide fuel pins. J.Nucl.Mat., 1993;204,252-260.
11. Kleykamp H, The chemical state of defective uranium-plutonium oxide fuel pins irradiated in sodium cooled reactors. J.Nucl.Mat., 1997;248,209-213.
12. Wilson RE, ERP JB, Chawla TC, Fauske HK, Kimont EL, Baldwin RD, Experimental evaluation of fission gas release in LMFBR subassemblies using an electrically heated test section with sodium as coolant. USA: Argonne National Laboratory, ANL- 8036 ;1973

13. ERP JB, Chawla TC, Fauske HK, An evaluation of pin-to-pin failure propagation due to fission gas release in fuel subassemblies of liquid-metal-cooled fast breeder reactors. Nucl. Eng. Des., 1974;31,128-150
14. Haga K, Kikuchi Y, Experimental investigation of coolability degradation by fission gas release into flowing sodium in a fuel bundle. Nucl. Technol., 1985;70,220-234